

## NUMERICAL MODELS FOR PREDICTING SPRING-BACK OF STAMPED TITANIUM ALLOY

KOREČEK David<sup>1</sup>, SOLFRONK Pavel<sup>2</sup>

<sup>1</sup>TUL - Technical University of Liberec, Liberec, Czech Republic, EU  
[david.korecek@tul.cz](mailto:david.korecek@tul.cz)<sup>1</sup>, [pavel.solfronk@tul.cz](mailto:pavel.solfronk@tul.cz)<sup>2</sup>

### Abstract

The paper is focused on the definition of a suitable material model of the titanium alloy, which is subsequent used for the numerical simulation of drawing process and the material spring-back by the FEM. Simulation of drawing process and subsequent spring-back was done in the environment of the simulation software PAM-STAMP 2G. In this simulation were used material models as Hill 48 and Vegter. These material models were defined in a version with isotropic and kinematic (Yoshida model) hardening of material. For a definition of these models, there was necessary to know the individual characteristics of material. Needed material characteristics were determined by the selected material tests. Results obtained by numerical simulations were compared with the results that have been measured by the real experiment of own stamping production.

**Keywords:** Drawing, spring-back of materials, numerical simulation, isotropic and kinematic hardening material model

### 1. INTRODUCTION

These days is titan and its alloy still more and more used in the technical practice as well as in the other branches of industry. Such reality is mainly given due to fact that there is put an accent on the lowering of mass of parts at keeping their mechanical properties as can be e.g. ultimate strength, ductility and other properties which characterize application possibilities for the given material. In light of its strength, titan offers the same results as common construction steel, but on the other hand it has much lower Young's modulus (approx. by 50%). Titan and its alloys have higher ratio of strength and density in comparison to the common construction steels and such fact makes possible to achieve a truly huge weight reduction by their utilization. These presumptions make from the titan and its alloys ideal material to be used not only in the engineering industry. However, lack of experience about its processing and production and mainly the much higher cost (compare to construction steels) force us to properly consider its application possibilities. [1]

The major aim of this paper was to determine proper material model for prediction spring-back of Ti-alloy and also methodology how to obtain necessary material properties which can be used for material model definition. Such material model was then used for the numerical simulation in the software PAM-STAMP 2G. As a testing material for the individual material tests and also the real experiment there was used titanium alloy Ti-CP AMS 4911 6Al-4V. The own obtaining of all needed material properties, definition of material models, numerical simulation and the real experiment are subsequently described in the following chapters.

### 2. METHODOLOGICAL BASES AND EXPERIMENTAL PART

In this chapter are described the individual material tests, which are necessary to obtain all needed material characteristics to define material model that is subsequently used in the numerical simulation.

#### 2.1. Standard static tensile test

Static tensile test was performed to obtain basic mechanical properties of the tested material. By means of the static tensile test was determined the proof yield strength  $R_{p0.2}$ , ultimate strength  $R_m$ , total ductility  $A_{80mm}$ ,

uniform ductility  $A_g$  and Young's modulus  $E$ . There were used flat tensile specimens and directions regarding the rolling direction in 0°, 45° and 90° (**Figure 1 - left**).

Static tensile test was performed on the testing device TIRA Test 2300 equipped with the common length gauge MFN-A-4-500. Subsequent evaluation was realized by means of software LabNET. Final values are given as arithmetic mean from 3 measurements in the **Table 1**.

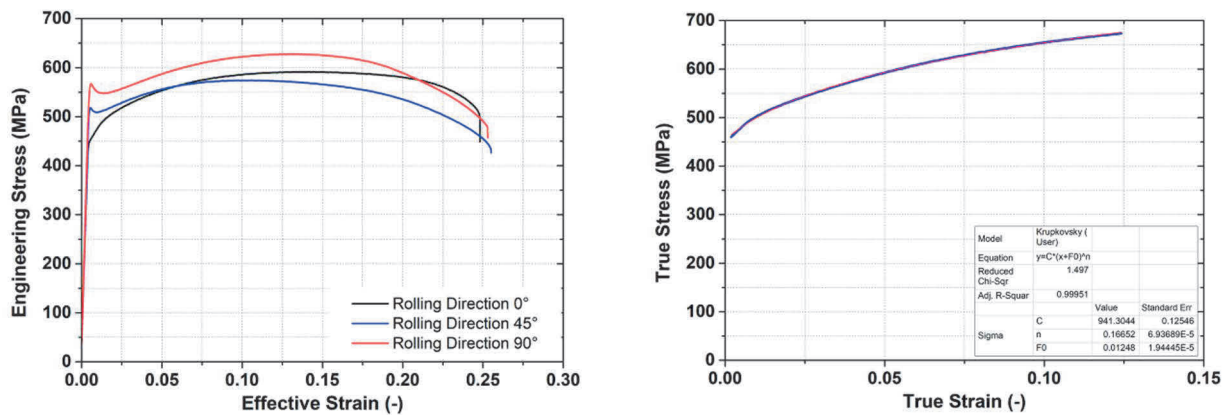


**Figure 1** Contractual diagram of tensile test (left) and approximation by Krupkovsky (right)

Moreover, approximation of the true stress-strain curve according to the Krupkovsky (**Figure 1 - right**) equation was done to determine the strength coefficient  $C$ , strain hardening exponent  $n$  and offset of deformation  $\phi_0$ . This approximation was performed in the software ORIGIN PRO 9 and results are also given in **Table 1**.

**Table 1** Overview of tensile test results and approximation coefficients

Rolling direction	Coefficient of normal anisotropy (-)	Yield strength (MPa)	Ultimate strength (MPa)	Uniform ductility (%)	Total ductility (%)	E (MPa)	Deformation for ultimate strength (-)	C (MPa)	n (-)	$\phi_0$ (-)
0°	0.8659	456.2	591.6	13.94	24.41	106199	0.12409	941.305	0.1665	0.0125
45°	2.3642	514.6	574.4	9.25	25.16	106199	0.08266	888.658	0.1515	0.0188
90°	2.6109	563.9	627.8	12.37	24.94	106199	0.11003	1031.737	0.1849	0.0192

**2.2. Determination of normal anisotropy coefficients**

Because testing material is not perfect monocrystal, but has a polycrystalline structure, it has different properties in the different directions, thereby the anisotropy takes place. To determine the normal anisotropy of tested material, there was also necessary to perform another test for different direction regarding the rolling direction - namely in the directions 0°, 45° a 90°. It was again the static tensile test, but in this case only up to the engineering strain  $\epsilon_{ENG} = 20\%$ . By means of this test was determined the normal anisotropy coefficient  $r_a$ . Such coefficient is computed from the initial and final dimensions of testing sample  $L_0$  and  $B_0$  as well as  $L_1$  and  $B_1$ . Results of normal anisotropy coefficients for different directions are given in **Table 1**.

**2.3. Hydraulic bulge test (HBT)**

Hydraulic bulge test (or equi-biaxial stretching by means of liquid pressure) was carried out with aim to simulate multi-axial loading for definition the Vegter material model. HBT was performed by hydraulic press CBA300/63

and jig for equi-biaxial loading of samples. The basic principle of test is to load sample uniformly along plane axis by oil pressure up to its failure. The whole test was scanned by the optical system ARAMIS.

Values measured by the HBT were subsequently used for computation both effective stress  $\sigma_i$  and effective strain  $\varphi_i$ . Moreover, these values were also used to determine approximation coefficient (again strength coefficient  $C$ , strain hardening exponent  $n$  and offset of deformation  $\varphi_0$ ) acc. to the Krupkovsky equation.

These quite important values ( $C$ ,  $n$  and  $\varphi_0$ ) are summarized in **Table 2**. Note that in this case they are for the another state of stress (equi-biaxial stretching) than that ones in **Table 1** (uniaxial tension). That's also a reason why are now these values much higher than from the common static tensile test. [2]

**Table 2** Overview of hydraulic bulge test results and approximation coefficients

$C$ (MPa)	$n$ (-)	$\varphi_0$ (-)	Deformation for ultimate strength (-)	$\varphi_{90}/\varphi_0$ (-)
1496.153	0.3117	0.0317	0.340	1.19015

**2.4. Plain strain tensile test**

Also so-called plain strain tensile test was used to determine the dependence of true stress on the true strain (another true stress-strain curve). For this test is valid one condition - deformation on the width direction equals zero (**Figure 2 - left**). Results of this plain strain tensile test (**Figure 2 - right**) are subsequently also used for definition the Vegter material model. Test was performed on the tensile test in the similar manner like in the case of the static tensile test. The whole course of test was recorded up to failure of the testing sample (in the notch area). [3]

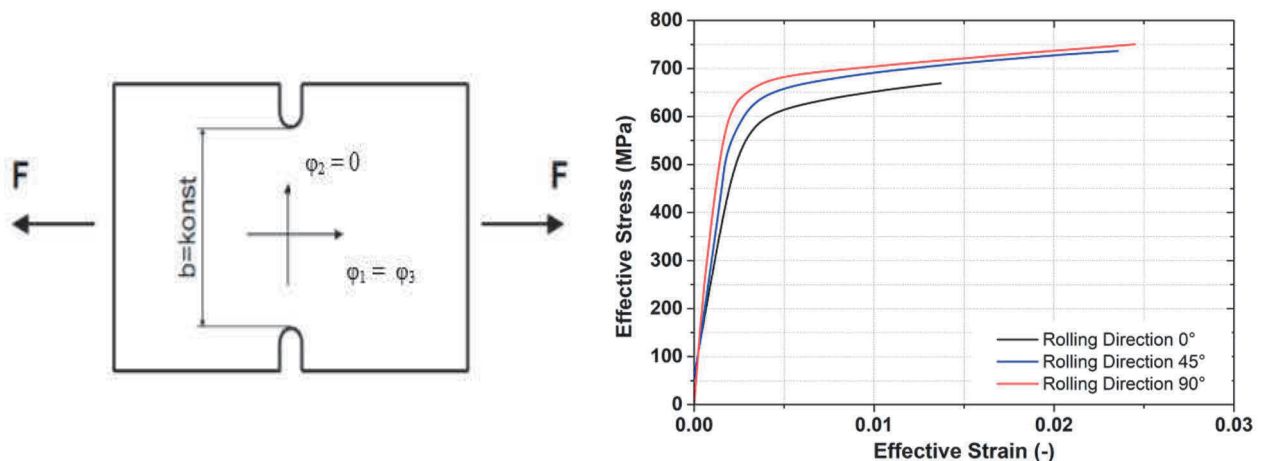


**Figure 2** Testing sample for the plain strain test (left) and stress-strain curve from the plain strain test (right)

**2.5. Cyclic test**

This test was used to determine courses of true stress and true strain during the cyclic loading. Such cyclic loading was done as a symmetrical variation of tensile and compressive loading of testing sample. The whole test was performed on the testing device TIRA Test 2300, now equipped with the special testing jaws (**Figure 3 - left**) which make possible such type of loading and prevent the sample from buckling. During this test takes effect also so-called Bauschinger effect (i.e. that yield strength varies due to the combined loading). [4]

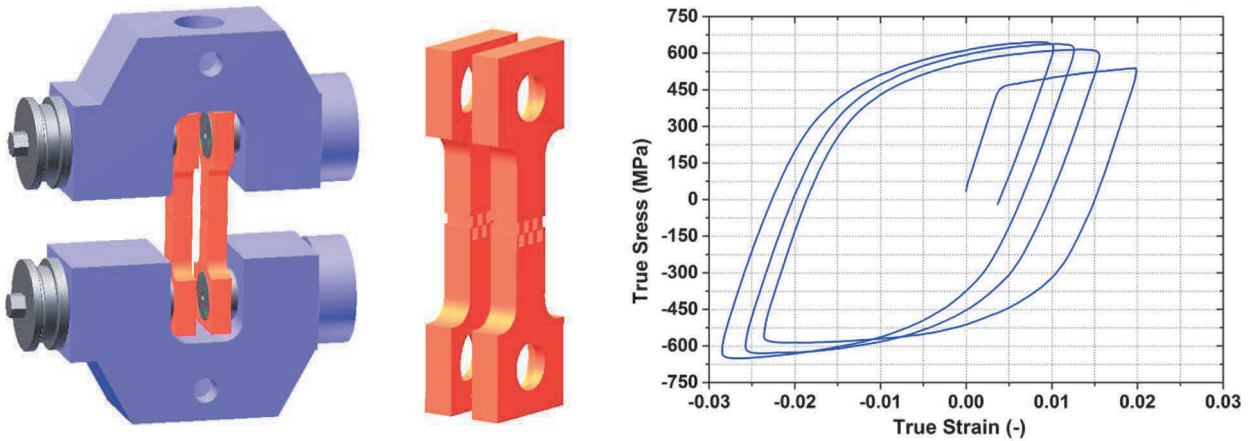


**Figure 3** Testing jaws for cyclic test (left) and stress-strain curve from the cyclic test (right)

### 2.6. Experimental measurement of the spring-back

The real bended sample was prepared by means of the bending tool which consists of die, punch and blank holder. Process of production for this sample is combination of bending and drawing. After production of the real sample, there was necessary to obtain its contour for its subsequent comparison with FEA. Such contour was scanned by means of 3D coordinate measuring machine. The experiment is shown in **Figure 4**.

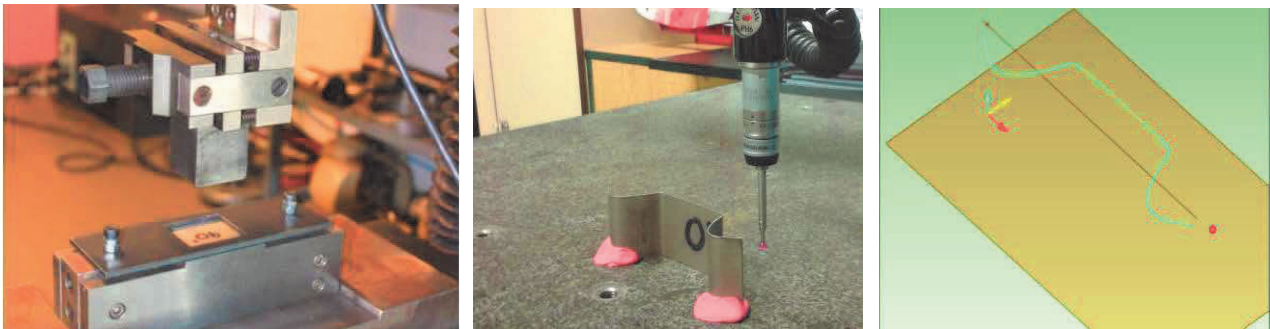


**Figure 4** Tool for production of real sample (left) and final contour of sample after experiment (right)

## 3. NUMERICAL SIMULATION OF THE SPRING-BACK

For the numerical simulation there were used two materials models termed as Hill 48 and Vegter. Both of these material models were applied as isotropic and kinematic (Yoshida) hardening of material.

### 3.1. Definition of the material models

Material model Hill 48 makes possible to compute with the directional dependence of the mechanical properties (anisotropy). Such material model is defined by Young's modulus  $E$ , Poisson's ratio  $\mu$ , density  $\rho$  and normal anisotropic coefficients in directions  $0^\circ$ ,  $45^\circ$  and  $90^\circ$ . Isotropic hardening of material (**Figure 5 - left**) is defined by the strain hardening mean curve that was measured from the static tensile test. Kinematic hardening of material (**Figure 5 - right**) is defined by the hysteresis loops that were obtained from the cyclic test.

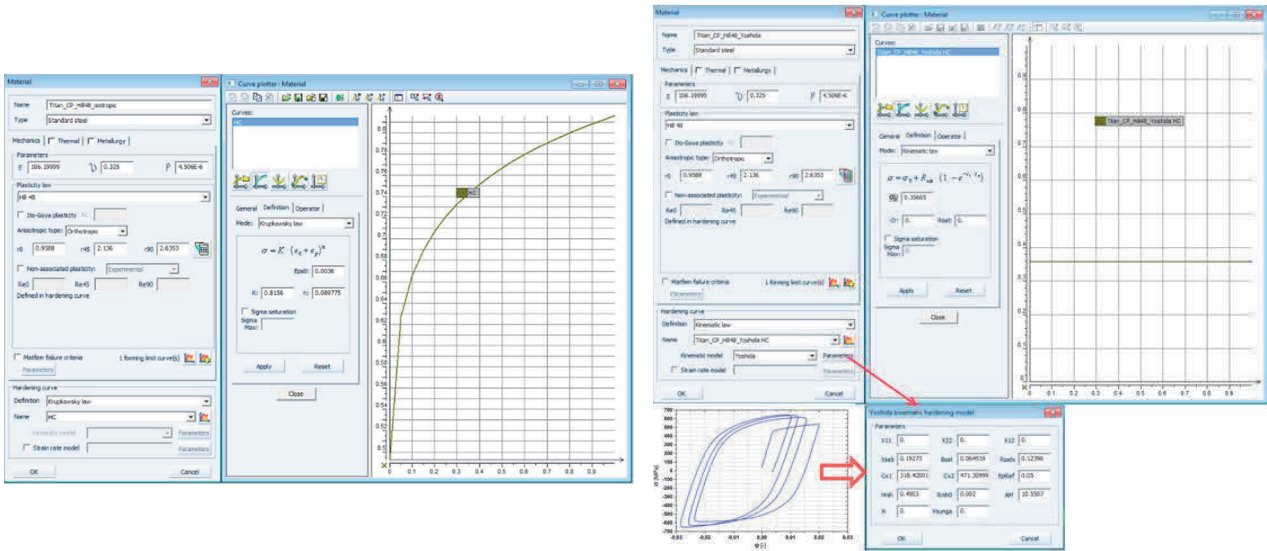


**Figure 5** Definition of material model Hill 48 as isotropic (left) and kinematic one (right)

For definition of the Vegter material model are used Young's modulus E, Poisson's ratio  $\mu$ , density  $\rho$  and normal anisotropic coefficients in directions  $0^\circ$ ,  $45^\circ$ ,  $90^\circ$  and biaxial anisotropy. Moreover, there are also used results from the plain strain test and HBT. Isotropic hardening of material (**Figure 6 - left**) is defined by the strain hardening mean curve that was measured from the static tensile test. And again, kinematic hardening of material (**Figure 6 - right**) is defined by the hysteresis loops that were obtained from the cyclic test. [3, 4]

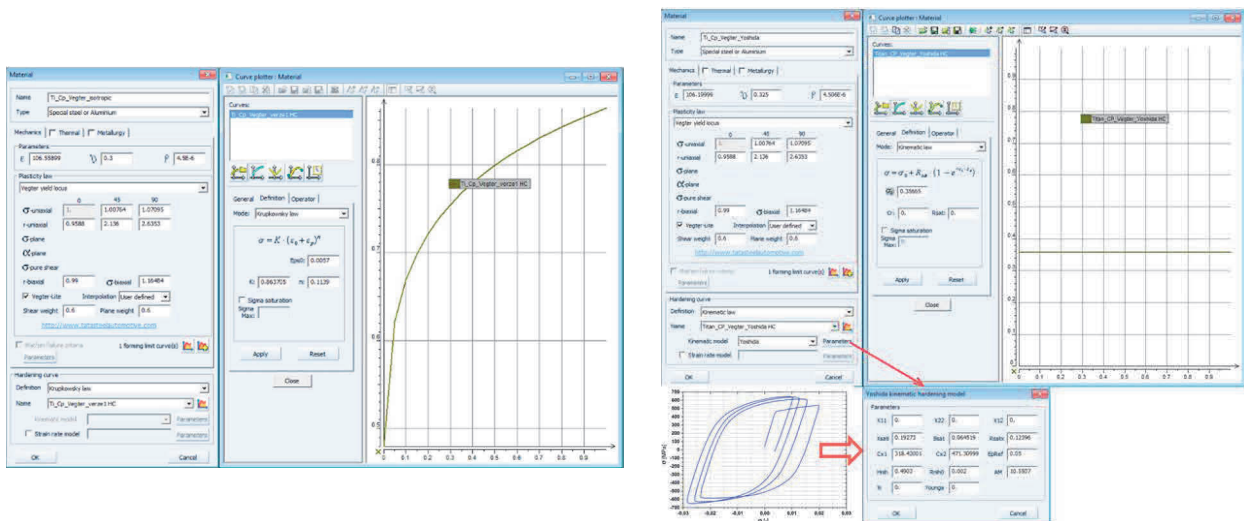


**Figure 6** Definition of material model Vegter as isotropic (left) and kinematic one (right)

### 3.2. Numerical simulation

Numerical simulation was performed by the software PAM-STAMP 2G which works on the basis of FEM. By such simulation there was simulated sheet metal forming process for sheet stamping which corresponds to the real experiment. After computation of FEM, it was exported a curve to define the contour of sheet.

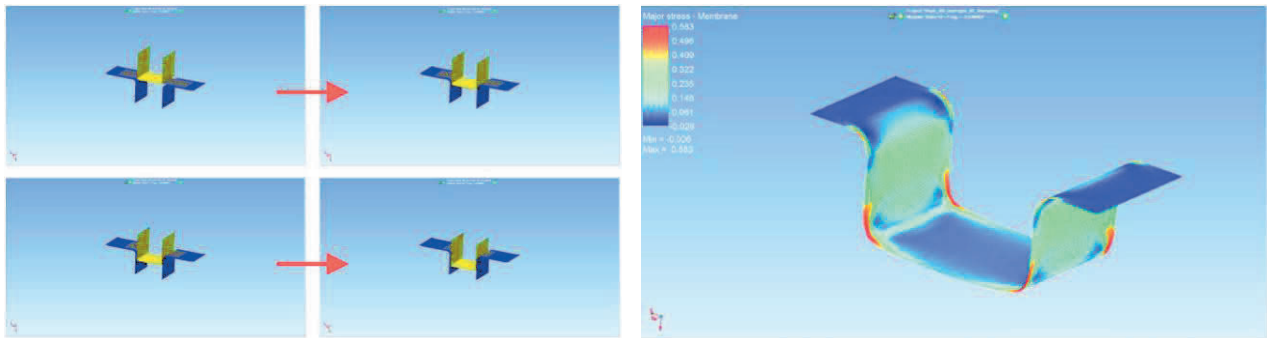


**Figure 7** Course of simulation in the software PAM STAMP 2G (left) and result of simulation (right)

### 3.3. Comparison of results from the real experiment and the numerical simulation (PAM-STAMP 2G)

In **Figure 8 (left)** is shown the comparison of the used material models Hill 48 and Vegter model. From this figure is evident that there aren't almost any differences between these two models. In **Figure 8 (right)** is shown the comparison of material model with the isotropic and kinematic hardening of material. There is already a visible difference between isotropic and kinematic hardening. Moreover, in **Figure 8 (right)** can be compare results from the FEM with the contour of the real sample.

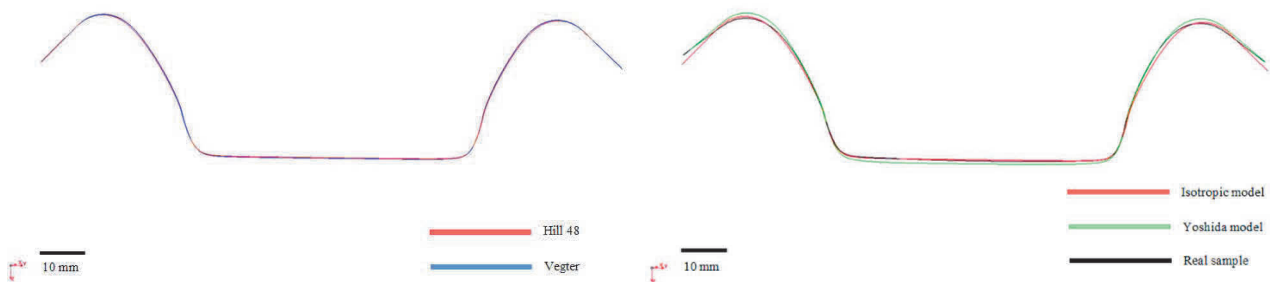


**Figure 8** Comparison of models Hill 48 and Vegter (left) and comparison of the isotropic hardening model, kinematic hardening model as well as the contour from the real sample (right)

## 4. CONCLUSION

The major aim of this paper was to determine and to define the material model, which can be used for the tested titanium alloy and numerical simulation by the software PAM-STAMP 2G. Because of that, there were chosen two material models termed as Hill 48 and Vegter. Both of these models were subsequently used with the isotropic and kinematic (here acc. to Yoshida model) hardening of material. Aim of the material model selection was to characterize deformation behavior of tested material with the highest accuracy. Material models were defined by means of material characteristics which were measured by the chosen materials tests (static tensile test, HBT, plain strain test, cyclic test).

There wasn't found any significant differences of shape contour at comparison Hill 48 and Vegter models. Some small differences were revealed at comparison of models with the isotropic and kinematic hardening of material. Here were found deviations in the spring-back angle of outer radii area and also in the total height of product. There was also performed the real sheet forming of tested titanium alloy Ti-CP AMS 4911 to have the contour of real product. From the final comparison of this real contour with the isotropic and kinematic material hardening models (see **Figure 8 - right**) is evident that the ideal material model would lie just on the boundary of these two models - because in light of the outer radii and spring-back angle of the outer parts of product is

real product closer to the kinematic (Yoshida) model, but in light of the total height of product is real product closer to the isotropic model.

## ACKNOWLEDGEMENTS

*This publication was written at the Technical University of Liberec as part of the Student Grant Contest "SGS 21179" with the support of the Specific University Research Grant, as provided by the Ministry of Education, Youth and Sports of the Czech Republic in the year 2017.*

## REFERENCES

- [1] MACHEK, V., SODOMKA, J. *Speciální kovové materiály*. Nauka o materiálu 3. část: Vyd. 1. V Praze: České vysoké učení technické, 2008. 118 p. ISBN 978-800-1042-120.
- [2] ASM HANDBOOK. *Volume 8 - Mechanical Testing and Evaluation*. 10th ed. Materials Park: ASM International, 2000. 998 p. ISBN 0-87170-389-0.
- [3] KOREČEK, D. *Finding a suitable material model for numerical simulation of sheet metal stamping pressed titanium alloy*. Technical University of Liberec, 2016.
- [4] YOSHIDA, F., UEMORI, T. A model of large-strain cyclic plasticity and its application to springback simulation. *International Journal of Mechanical Sciences*, October 2003, Vol. 45, No. 10., pp 1687-1702. ISSN 0020-7403.